

Magnification of conic mirror reflectometers

Keith A. Snail and Leonard M. Hanssen

Conic mirror reflectometers are used to measure the diffuse reflectance and total integrated scatter of surfaces. In spite of the long history of using conic mirrors for these purposes, the maximum magnification of the three primary types of conic mirror (hemisphere, hemiellipsoid, and dual paraboloid) had not been compared quantitatively. To our knowledge, an exact magnification formula has not been published for any of the three primary conic mirrors. The maximum magnification is needed for proper sizing of detectors and radiation sources used with reflectometers. Exact analytical expressions for the maximum magnification of a Coblentz hemisphere, a hemiellipsoid, and a dual-paraboloid mirror system are derived and compared.

OCIS codes: 120.5820, 120.4570, 220.2740, 120.5700, 120.3150, 080.2740.

1. Introduction

Accurate measurements of the spectral reflectance of diffusing surfaces are important to many scientific and engineering disciplines. Before 1980, conic mirror reflectometers based on hemispherical,^{1,2} dual-paraboloidal,³ and hemiellipsoidal⁴⁻⁸ mirrors were the most commonly used instruments for measuring the diffuse reflectance of solid opaque samples in the mid- to far-infrared wavelength range (2–60 μm). Coblentz hemispheres⁹ have also been frequently used to measure the total integrated scatter¹⁰ of specular surfaces. Following the advent of more Lambertian, high-reflectance roughened gold coatings¹¹⁻¹³ in the 1970's and 1980's, diffuse reflectance measurements in the mid-infrared wavelength range (2–14 μm) are increasingly being performed with integrating spheres. The development of infrared integrating spheres has been accelerated by the extensive body of work on visible integrating spheres from the first half of this century. In contrast, conic mirror devices were rarely used in the visible because of the constraints imposed by optical scatter. As a consequence, the literature on conic mirror reflectometers is limited and incomplete compared with that on integrating spheres.

A recent joint project between the Naval Research Laboratory and the National Institute of Standards and Technology was aimed at improving the instru-

mentation used to measure diffuse reflectance in the infrared to facilitate the development of infrared diffuse reflectance standards. As a result of that effort, a more comprehensive understanding of the measurement errors associated with conic mirror reflectometers was developed.¹⁴ For diffuse reflectometers operated in the directional-hemispherical mode and for typical total integrated scatter instruments, one needs to know the maximum magnification in order to size the detector to collect all the scattered light from the sample. For conic mirror reflectometers operated in the hemispherical-directional mode, one needs to know the maximum magnification to determine the minimum radiation source size required to ensure uniform Lambertian illumination of the sample. In this paper exact analytical expressions for the maximum magnification are derived for a circular source for a Coblentz hemisphere (derived by Snail), a hemiellipsoid (derived by Snail), and a dual-paraboloidal system (derived by Hanssen). These new formulas are compared with one another, with ray-trace results, and with the well-known approximate expression for the maximum magnification of a hemiellipsoidal mirror.

2. Terminology

The two most common measurement geometries used for performing diffuse reflectance measurements are the directional-hemispherical ($\theta/2\pi$) and the hemispherical-directional ($2\pi/\theta$) geometries. In this notation the first term in parentheses refers to the geometry of illumination, whereas the second term refers to the geometry of light collection. The directional-hemispherical reflectance is the fraction of flux incident within a small solid angle about the

K. A. Snail is with the Naval Research Laboratory, Washington, D.C. 20375-5320. L. M. Hanssen is with the National Institute of Standards and Technology, Gaithersburg, Maryland 20899.

Received 31 October 1997; revised manuscript received 13 March 1998.

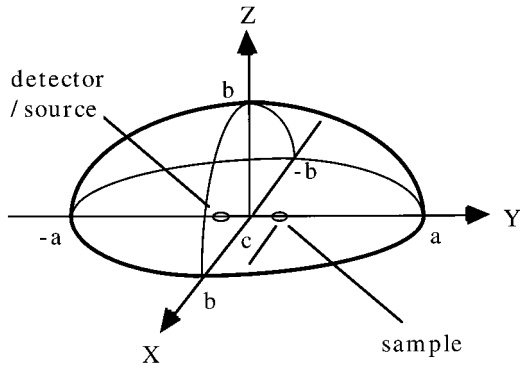


Fig. 1. Geometry of a typical hemispheroidal mirror reflectometer.

direction θ that is reflected into the hemisphere above the surface and is denoted by the letter ρ . By the Helmholtz reciprocity principle,^{15,16} a measurement in the $(2\pi/\theta)$ geometry will yield the same reflectance value as in the $(\theta/2\pi)$ geometry. In practice, actual measurement geometries only approximate the ideal geometry because of the presence of ports and other factors. The directional-hemispherical reflectance is composed of a diffuse (ρ_d) and a specular or regular (ρ_r) component. A complete list of symbols with definitions can be found in Appendix A.

The linear magnification of conic mirror reflectometers is usually defined as the derivative of an image coordinate with respect to the analogous object coordinate.¹⁷ This definition can lead to erroneous results for finite-sized objects because of the presence of aberrations. A more appropriate definition is based on the edge ray principle of nonimaging optics. This approach uses one or two extremal rays that are launched from the edge(s) of the object. Two edge rays are required for the hemisphere, whereas the dual-paraboloid requires only one because of its azimuthal symmetry about the sample normal. Hemispheroidal reflectometers can be designed with azimuthal symmetry about the sample normal.⁴ In that case, one edge ray is needed, whereas for designs with the sample normal orthogonal to the major axis, two edge rays are needed. Rays that intersect the edge of the conic mirror will typically determine the maximum magnification of the reflectometer. One exception to this rule is the dual-paraboloid case in which the base planes of the paraboloids are not coplanar. This case is not analyzed in this paper.

3. Magnification Formulas

The arrangement of a typical hemispheroidal mirror reflectometer is shown in Fig. 1. For a $(\theta/2\pi)$ geometry reflectometer, the detector is located at one (effective) focus and the source is located externally, whereas in the $(2\pi/\theta)$ geometry the source is at a focus and the detector is external. The optics (not shown in the figure) used to illuminate $(\theta/2\pi)$ geometry or view $(2\pi/\theta)$ geometry the sample can be suspended either inside the conic mirror or outside a port in the conic mirror. The semimajor axis length is

denoted a , the semiminor axis length b , the focal distance c , and the eccentricity $\epsilon (=c/a)$. For a hemispherical mirror, $a = b = R$, where R is the radius of the hemisphere. The sample is assumed to be centered at $Y = c$ for the hemispheroidal and at the position $Y = c'$ (not shown) for the hemisphere. A quantity $\epsilon' (=c'/R)$ analogous to the eccentricity will be defined for the hemisphere. Because of aberrations in the image, a circular detector's center should optimally be placed at a position $Y < -c$ for the hemispheroidal and $Y < -c'$ for the hemisphere.¹⁷

The image size on the detector $(\theta/2\pi)$ geometry depends on the scattering properties of the sample. For Lambertian samples, the magnification will be a maximum. The magnification will be characterized in terms of a longitudinal value along the y axis (M_y) and a transverse value along the x axis (M_x). Knowledge of the maximum linear magnification of a hemispheroidal or a dual-paraboloidal mirror is required for sizing a reflectometer's detector $(\theta/2\pi)$ geometry to collect all the reflected radiation or for sizing the radiation source $(2\pi/\theta)$ geometry to illuminate the sample uniformly.¹⁸ When an analytical solution is not available, the maximum magnification of a conic mirror reflectometer can be determined by ray tracing. In many cases the tracing of extremal rays from the two points defined by the intersection of a circular beam spot on the sample with the major axis of the reflectometer will suffice to determine the maximum linear magnification. One would like to use a conic mirror with the smallest magnification possible to minimize the source size $(2\pi/\theta)$ or the detector size $(\theta/2\pi)$ geometry and hence the detector noise. For most reflectometers the detector noise will scale¹⁹ as $\sqrt{A_D}$, where A_D is the detector area.

A. Hemisphere

The maximum linear magnification of a hemispherical mirror along the axis containing the detector-source and sample is given approximately¹⁷ by

$$M_{y,HS} \cong \frac{1}{(1 - 2\epsilon')^2}. \quad (1)$$

However, because of spherical aberration, relation (1) significantly underestimates the true magnification for $\epsilon' > 2r_s/R$, where r_s is equal to the viewed radius $(2\pi/\theta)$ geometry or to the beam spot radius $(\theta/2\pi)$ geometry on the sample. From a ray-trace analysis it was determined that for $r_s/R = 0.05$ and $\epsilon' = 0.2$ the actual magnification is 38% greater than that predicted by relation (1). For $\epsilon' = 0.1$ the actual magnification is 8% greater than the value predicted by relation (1). An alternative expression that takes spherical aberration into account is derived in Appendix B. The exact longitudinal magnification of a hemispherical mirror is given by

$$M_{y,HS} = \frac{\frac{2\epsilon'^2}{\delta'} - (2\delta' - 1)}{(2\delta' - 1)^2 - 4\epsilon'^2}, \quad (2)$$

where $\delta' = (r_s/R)$. Note that as δ' goes to zero, $M_{y,HS}$ goes to infinity, as expected. If the sample is fully illuminated, then $\epsilon' = \delta'$ corresponds to the sample and the detector just touching at $y = 0$. Under this condition, Eq. (2) reduces to $1/(1 - 4\epsilon')$. For $(2\pi/\theta)$ geometry instruments the ratio of the source radius to the viewed sample radius should be equal to or greater than the maximum magnification to ensure uniform illumination over the viewed area on the sample. In this case the sample will be overilluminated.

The maximum linear magnification along the x axis, M_x , in Fig. 1 is equal to the square root of M_y for both the hemisphere and the hemiellipsoid.¹⁷ Hence, when one is using a monochromator with a spheroidal mirror, one can minimize the detector ($\theta/2\pi$ geometry) or the source ($2\pi/\theta$ geometry) area by aligning the image of the monochromator's slit on the sample so the long axis is perpendicular to the spheroidal mirror axis containing the sample and the detector or source.

B. Hemiellipsoid

Brandenberg¹⁷ has shown that the maximum linear magnification along the semimajor axis of a hemiellipsoidal mirror is approximately equal to

$$M_{y,HE} \cong \left(\frac{1 + \epsilon}{1 - \epsilon} \right)^2. \quad (3)$$

Ray-tracing analyses^{20,21} indicate that, for a circular source, relation (3) sets a lower bound for the linear magnification, with an error of less than 0.7% for $\epsilon < 0.3$ and $r_s/a = 0.02$. For $r_s/a = 0.04$, the error is less than 2% for $\epsilon < 0.25$. Relation (3) can be written as a power series in ϵ ($M_{y,HE} = 1 + 4\epsilon + 8\epsilon^2 + 12\epsilon^3 + \dots$). The maximum magnification of a hemisphere [Eq. (2)] can also be expanded in a power series when $\delta' = \epsilon'$ [in this case $M_{y,HS}$ reduces to $1/(1 - 4\epsilon)$]. The resultant series ($M_{y,HS} = 1 + 4\epsilon' + 16\epsilon'^2 + 64\epsilon'^3 + \dots$) differs from the hemiellipsoid result in the second-order and higher terms.

It is also possible to derive an exact expression for the maximum magnification of a hemiellipsoidal mirror. Starting with Eq. (17) of Ref. 17 and setting $X = 0$ and $Y = a$, one can obtain an expression for $M_{y,HE} = (Y_2' - Y_2)/Y_1' - Y_1$, where $Y_1' = c + r_s$ and $Y_1 = c - r_s$. This expression can be simplified to yield the following result:

$$M_{y,HE} = \frac{(1 - \epsilon)^2}{(1 - \epsilon)^2 - \left(\frac{2\delta}{1 - \epsilon} \right)}, \quad (4)$$

where $\delta = r_s/a$. For $r_s = 0.05$ and $\epsilon = 0.1$ the hemiellipsoid magnification predicted by Eq. (4) is approximately 1.5% higher than that predicted by relation (3).

C. Dual Paraboloid

The cross section of a dual-paraboloidal mirror reflectometer is shown in Fig. 2. We assume that the axes of the two paraboloids are collinear and that the

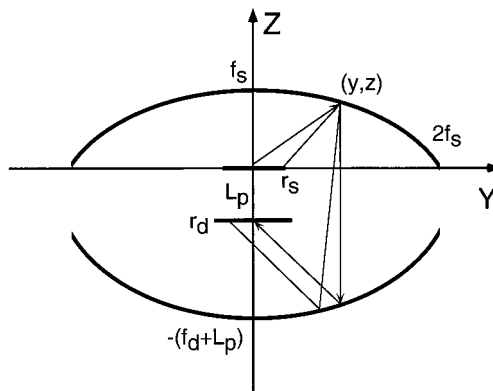


Fig. 2. Geometry of a typical dual-paraboloidal mirror reflectometer.

detector or source and the sample are centered on the axes. The paraboloids have focal lengths f_s and f_d , and the separation between the sample and the detector or source is equal to L_p .

For a dual-paraboloidal mirror reflectometer the exact maximum magnification factor is derived in Appendix C. When the focal lengths of the two paraboloids are equal, $f = f_s = f_d$, and the separation distance is $L_p = 0$, the magnification can be determined from an edge ray analysis as θ approaches 90° . If we define a quantity $\epsilon'' = r_s/2f$, then the maximum linear magnification of a dual-paraboloidal mirror as derived in Appendix C is given by

$$M_{y,DP} = \frac{1}{(1 - 2\epsilon'')}. \quad (5)$$

This equation was confirmed for a specific geometry by use of a ray-tracing code, ASAP.²¹ We can compare this result directly with the hemispherical and hemiellipsoidal factors by expansion: $M_{y,DP} = 1 + 2\epsilon'' + 4\epsilon''^2 + 8\epsilon''^3 + \dots$. Note that if we were to redefine ϵ'' as $r_s/4f$, then $M_{y,DP} = M_{y,HS}$ ($\delta' = \epsilon'$) and all three mirror types could have their magnification described (to first order in ϵ) as $M_y \approx 1 + 4\epsilon$. However, we prefer the earlier definition of ϵ'' , as discussed further in Section 4. Because of the circular symmetry of the dual-paraboloidal geometry, the magnification of a circular beam spot centered on a diffuse sample can be characterized by a single value, $M_{x,DP} = M_{y,DP}$.

Two other properties of the dual-paraboloidal design are worth mentioning. First, if f_d is greater than f_s , the maximum incidence angle on the detector is reduced and consequently the magnification increases to conserve étendue. Second, the larger range of incidence angles ($0-45^\circ$) on the dual-paraboloids compared with those on the hemisphere and the hemiellipsoid may introduce a polarization-related bias that is not discussed in this paper.

A comparison of the maximum magnification of the three primary types of conic mirror reflectometers is shown in Fig. 3, as calculated from Eqs. (2), (4), and (5). The magnifications of the hemiellipsoid and the dual-paraboloid are significantly less than that of the

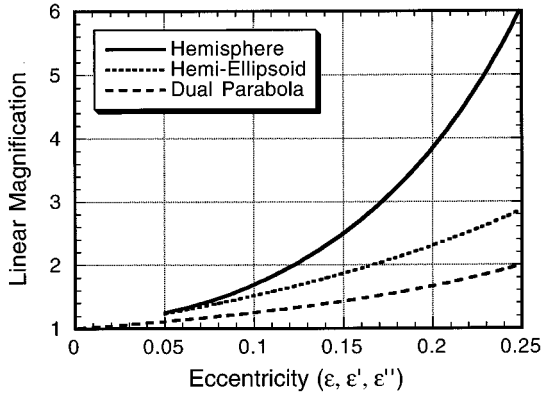


Fig. 3. Maximum linear magnification for hemispherical, hemiellipsoidal, and dual-paraboloidal mirrors for the geometries discussed in the text and as calculated from Eqs. (2), (4), and (5). For the hemisphere (hemiellipsoid) the ratio of the beam spot radius to the hemisphere radius (hemiellipsoid semimajor axis length) was set at 0.05.

hemisphere for $\varepsilon = \varepsilon' = \varepsilon'' > 0.1$. For $\varepsilon = \varepsilon' < 0.08$ the incremental advantage of using a hemiellipsoid over a hemisphere is small. Realistically, one may not be able to set $\varepsilon = \varepsilon' = \varepsilon''$ for comparison purposes. For instance, if the largest physical dimensions of the conic mirrors are set equal ($R = a = 2f_s$) and if the detector size is fixed, the beam spot size ($\theta/2\pi$) on the sample required to illuminate the detector fully will be different for each conic mirror type. Hence one may have $\varepsilon'' < \varepsilon = \varepsilon'$.

The magnifications of the hemisphere and the hemiellipsoidal mirrors are not shown in Fig. 3 for $\varepsilon' < \delta'$ and $\varepsilon < \delta$ because this type of magnification would correspond to the detector ($\theta/2\pi$ geometry) or source ($2\pi/\theta$ geometry) occupying the same physical space as the sample. Paschen²² placed a detector with a diffuse surface at the center of a hemispherical mirror to decrease its reflectance. With this configuration ($\varepsilon' = 0$) the ratio of the beam spot radius to the detector radius should be equal to $(1 - 2\delta)$ to reimage all the nonabsorbed radiation onto the detector after the first reflection from the hemispherical mirror.

4. Summary and Conclusions

Exact analytical formulas for the maximum magnification of a Coblentz hemisphere, a hemiellipsoid, and a dual-paraboloidal mirror system have been presented. For low eccentricities ($\varepsilon, \varepsilon' < 0.08$) and moderately sized beam spot diameters the maximum magnifications of the hemisphere and the hemiellipsoid differ by only a small amount. The maximum magnification of a dual-paraboloidal system is significantly less than that of a hemisphere and moderately less than that of a hemiellipsoid. An important consideration is the definition of ε' and ε'' for comparison purposes. We defined them such that the open diameter for all three mirrors would be the same. We believe that this is a reasonable approach.

For the purpose of selecting one conic mirror over

another, the signal-to-noise ratio is a more useful figure of merit than the maximum magnification. In comparing the signal-to-noise ratios of the three designs, one must consider the changes in signal level associated with the beam spot size variations as well as the lower throughput of the dual-paraboloidal design that is due to self-shadowing by the sample and the second reflection on the detector paraboloid. Further evaluations of the maximum magnification factor for dual paraboloids with different focal lengths and separations are under way.

Appendix A: Definitions of Symbols Used

- a Hemiellipsoid semimajor axis length,
- b Hemiellipsoid semiminor axis length,
- c Hemiellipsoid focal distance,
- c' Hemisphere sample center position,
- δ Hemiellipsoid dimensionless parameter ($\equiv r_s/R$),
- δ' Hemisphere dimensionless parameter ($\equiv r_s/a$),
- ε Hemiellipsoid eccentricity ($\equiv c/a$),
- ε' Hemisphere eccentricity ($\equiv c'/R$),
- ε'' Dual-paraboloid eccentricity ($\equiv r_s/2f_s$),
- f Focal length of paraboloid,
- f_d Focal length of detector paraboloid,
- f_s Focal length of sample paraboloid,
- L_p Separation distance of dual paraboloids,
- $M_{y,HS}$ Maximum linear magnification of hemisphere along the y axis,
- $M_{y,HE}$ Maximum linear magnification of hemiellipsoid along the y axis,
- $M_{y,DP}$ Maximum linear magnification of dual paraboloid,
- ρ Directional hemispherical ($\theta/2\pi$) reflectance, composed of diffuse (ρ_d) and specular (ρ_r) components,
- ρ_d Diffuse reflectance ($\equiv \rho - \rho_r$),
- ρ_r Specular or regular reflectance ($\equiv \rho - \rho_d$),
- r_s Beam spot radius ($\theta/2\pi$) or viewed radius ($2\pi/\theta$) on the sample,
- r_d Detector radius,
- R Hemisphere radius,
- θ Polar angle.

Appendix B: Magnification of a Hemispherical Mirror

To determine the magnification of a hemispherical mirror one must first express the coordinates of a ray's intersection with the image plane (x_3, y_3) in terms of both the ray's starting coordinates in the object plane (x_1, y_1) and the ray's intersection point with the hemisphere (x_2, y_2). The hemispherical mirror shown in Fig. 4 illustrates the relationship of these coordinates.

According to Snell's law, the unit vector at point (x_2, y_2) that is pointing toward (x_3, y_3) is given by

$$\hat{s}_2 = \hat{s}_1 - 2(\hat{s}_1 \cdot \hat{n})\hat{n}, \quad (\text{B1})$$

where \hat{n} is the unit vector normal to the hemisphere at point (x_2, y_2) and \hat{s}_1 is the unit vector at point

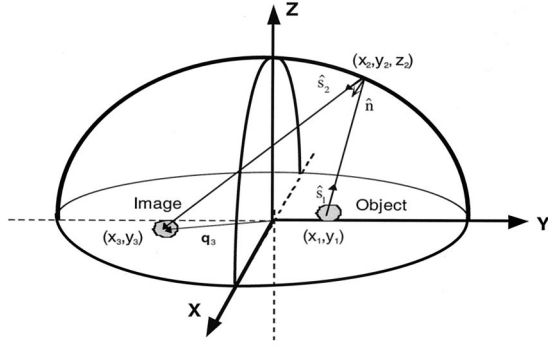


Fig. 4. Geometrical arrangement of a typical hemispherical mirror.

(x_1, y_1) that is pointing toward (x_2, y_2) . The vector \mathbf{q}_3 is equal to the sum of vector \mathbf{q}_2 (not shown) and $d_{23}\hat{s}_2$, where d_{23} is the distance from (x_2, y_2) to (x_3, y_3) . This equality yields the following three equations:

$$x_3 = x_2 + d_{23} \left[\frac{x_2 - x_1}{d_{12}} + \frac{2(\hat{s}_1 \cdot \hat{n})x_2}{R} \right], \quad (\text{B2})$$

$$y_3 = y_2 + d_{23} \left[\frac{y_2 - y_1}{d_{12}} + \frac{2(\hat{s}_1 \cdot \hat{n})y_2}{R} \right], \quad (\text{B3})$$

$$0 = z_2 + d_{23} \left[\frac{z_2}{d_{12}} + \frac{2(\hat{s}_1 \cdot \hat{n})z_2}{R} \right], \quad (\text{B4})$$

where d_{12} is the distance from (x_1, y_1) to (x_2, y_2) and $(\hat{s}_1 \cdot \hat{n})$ is equal to $[(x_2x_1 + y_2y_1) - R^2]/(Rd_{12})$. Solving Eq. (B4) for d_{23} and substituting the result into Eqs. (B2) and (B3) yields the following expressions:

$$x_3 = \frac{x_1 R^2}{2(x_2x_1 + y_2y_1) - R^2}, \quad (\text{B5})$$

$$y_3 = \frac{y_1 R^2}{2(x_2x_1 + y_2y_1) - R^2}. \quad (\text{B6})$$

For a circular beam spot on the sample, the maximum magnification of the image can be determined from two rays that originate on the axis that bisects the object and the image. If we choose that axis to be the y axis in Fig. 4, then the image length on the y axis is given by $[y_3(y_1 = -c' - r_s, y_2 = -R) - y_3(y_1 = -c' + r_s, y_2 = R)]$, where r_s is the radius of the beam spot. Dividing the image length by $2r_s$ and simplifying yield Eq. (2).

Appendix C: Maximum Linear Magnification of a Dual-Paraboloidal Mirror

To determine the magnification of a dual-paraboloidal mirror we proceed as in Appendix B to express the coordinates of a ray's intersection with the image plane (x_4, y_4) in terms of both the ray's starting coordinates in the object plane (x_1, y_1) and the ray's intersection points with the paraboloids (x_2, y_2, z_2) and (x_3, y_3, z_3) . The dual-paraboloidal mirror shown in Fig. 5 illustrates the relationship of these coordinates.

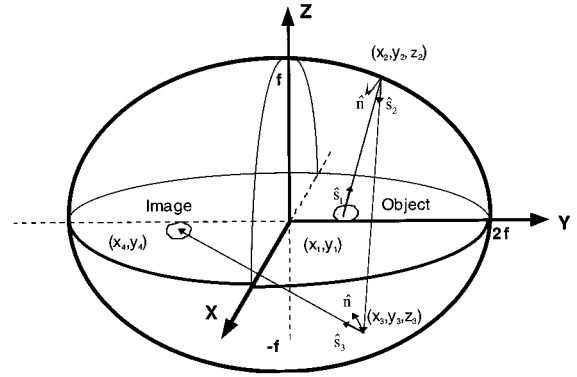


Fig. 5. Imaging of rays in a dual-paraboloidal mirror system with paraboloids of identical focal length ($f = f_s = f_d$) and coincident foci. Points at (x_2, y_2, z_2) and (x_3, y_3, z_3) are reflection points on the two paraboloids, whereas points (x_1, y_1) and (x_4, y_4) are the starting and end points, respectively.

We begin with a ray leaving point (x_1, y_1) with direction vector \hat{s}_1 :

$$\hat{s}_1 = \cos(\alpha)\hat{x} + \cos(\beta)\hat{y} + \cos(\gamma)\hat{z}, \quad (\text{C1})$$

where α , β , and γ are the angles between \hat{s}_1 and the coordinate axes.

Without loss of generality, we select $y_1 = 0$ (this is equivalent to a rotation of the coordinate system about the z axis). Because $y_1 = 0$, y_4 will also be 0, so the s_{1y} component should not have an effect on the value of x_4 or hence on the maximum magnification. For simplification, then, we can further select $\beta = \pi/2$. The general equation of the line through a point (x_0, y_0, z_0) and along a unit vector \hat{s} is

$$\frac{x - x_0}{s_x} = \frac{y - y_0}{s_y} = \frac{z - z_0}{s_z}, \quad (\text{C2})$$

then the line along \hat{s}_1 , through point $(x_1, 0, 0)$ is

$$\frac{x - x_1}{\cos(\alpha)} = \frac{z}{\cos(\pi/2 - \alpha)}. \quad (\text{C3})$$

The intersection point of the line with the upper paraboloid is (x_2, y_2, z_2) , given by the intersection of the line [Eq. (C4)] and the paraboloid [Eq. (C5)]:

$$x_2 - x_1 \cos(\alpha) = \frac{z_2}{\sin(\alpha)}, \quad (\text{C4})$$

$$z_2 = f - \frac{x_2^2}{4f}. \quad (\text{C5})$$

The unit vector corresponding to the reflected ray \hat{s}_2 is given by

$$\hat{s}_2 = \hat{s}_1 - 2(\hat{s}_1 \cdot \hat{n})\hat{n}, \quad (\text{C6})$$

where

$$\hat{n} = \left(-\frac{\partial z}{\partial x} \hat{x} + \hat{z} \right) / \left[\left(\frac{\partial z}{\partial x} \right)^2 + 1 \right]^{1/2} \quad (\text{C7a})$$

or

$$\hat{n} = \left(\frac{x_2}{2f} \hat{x} + \hat{z} \right) / \left[\left(\frac{x_2}{2f} \right)^2 + 1 \right]^{1/2} \quad (C7b)$$

and

$$\hat{s}_1 \cdot \hat{n} = \left[\frac{\cos(\alpha)x_2}{2f} + \cos(\pi/2 - \alpha) \right] / \left[\left(\frac{x_2}{2f} \right)^2 + 1 \right]^{1/2}. \quad (C8)$$

The components of \hat{s}_2 become

$$s_{2x} = \cos(\alpha) - \frac{x_2}{f} \left[\frac{\cos(\alpha)x_2}{2f} + \cos(\pi/2 - \alpha) \right] / \left[\left(\frac{x_2}{2f} \right)^2 + 1 \right], \quad (C9a)$$

$$s_{2y} = 0, \quad (C9b)$$

$$s_{2z} = \cos(\pi/2 - \alpha) - 2 \left[\frac{\cos(\alpha)x_2}{2f} + \cos(\pi/2 - \alpha) \right] / \left[\left(\frac{x_2}{2f} \right)^2 + 1 \right]. \quad (C9c)$$

Plugging Eqs. (C9) into Eq. (C2) gives us the equation for the line of the reflected ray:

$$\frac{x - x_2}{s_{2x}} = \frac{z - z_2}{s_{2z}}. \quad (C10)$$

The intersection point of this line with the lower parabola is (x_3, y_3, z_3) , given by the intersection of the line [Eq. (C11)] and the paraboloid [Eq. (C12)]:

$$\frac{x_3 - x_2}{s_{2x}} = \frac{z_3 - z_2}{s_{2z}}, \quad (C11)$$

$$z_3 = \frac{x_3^2}{4f} - f. \quad (C12)$$

The unit vector corresponding to the reflected ray \hat{s}_3 is given by

$$\hat{s}_3 = \hat{s}_2 - 2(\hat{s}_2 \cdot \hat{n})\hat{n}, \quad (C13)$$

where

$$\hat{n} = \left(\frac{x_3}{2f} \hat{x} - \hat{z} \right) / \left[\left(\frac{x_3}{2f} \right)^2 + 1 \right]^{1/2}, \quad (C14)$$

$$\hat{s}_2 \cdot \hat{n} = \left(\frac{s_{2x}x_3}{2f} - s_{2z} \right) / \left[\left(\frac{x_3}{2f} \right)^2 + 1 \right]^{1/2}, \quad (C15)$$

$$s_{3x} = s_{2x} - \frac{x_3}{f} \left(\frac{s_{2x}x_3}{2f} - s_{2z} \right) / \left[\left(\frac{x_3}{2f} \right)^2 + 1 \right], \quad (C16a)$$

$$s_{3y} = 0, \quad (C16b)$$

$$s_{3z} = s_{2z} + 2 \left(\frac{s_{2x}x_3}{2f} - s_{2z} \right) / \left[\left(\frac{x_3}{2f} \right)^2 + 1 \right]. \quad (C16c)$$

Finally, the intersection of the line formed by (x_3, y_3, z_3) and Eqs. (C16), and the base plane ($z = 0$), gives us the final point $(x_4, y_4, 0)$:

$$\frac{x_4 - x_3}{s_{3x}} = \frac{-z_3}{s_{3z}}. \quad (C17)$$

Then we set up the following equations to solve:

$$x_4 = x_3 - z_3 \frac{s_{3x}}{s_{3z}}, \quad (C18a)$$

$$y_4 = 0. \quad (C18b)$$

Combining Eqs. (C18), (C16), (C12), (C11), (C9), (C5), and (C4) gives the position (x_4, y_4) in terms of (x_1, y_1) and α . This process was carried out with the algebraic calculation features of the Mathematica 3.0 program on a Power Macintosh computer. The exact sequence of steps in the program is as follows: (a) Solve Eqs. (C1), (C2), and (C3) for (x_2, y_2, z_2) ; (b) plug (x_2, y_2, z_2) into Eqs. (C4)–(C6); (c) solve for (s_{2x}, s_{2y}, s_{2z}) ; (d) plug the result into Eqs. (C7) and (C8); (e) solve Eqs. (C7)–(C9) for (x_3, y_3, z_3) ; (f) plug the result into Eqs. (C10)–(C12); (g) solve for (s_{3x}, s_{3y}, s_{3z}) ; (h) plug the result into Eqs. (C13) and (C14); (i) solve for (x_4, y_4) . On two occasions when we solved the quadratic equations describing the two paraboloids, a pair of solutions resulted. Each of these was carried out to yield a solution for x_4 . The solution shown below corresponds to the maximum magnification for rays leaving a positive x_1 along the x axis. For rays leaving a positive x_1 in the negative x direction the $-$ in the denominator is replaced with a $+$. The other solutions are nonphysical. To reduce the resulting expression for x_4 to the value for maximum magnification we performed a series expansion in powers of α about $\alpha = 0$. This was done separately for the numerator (N) and the denominator (D) of the analytical form of x_4 :

$$N(x_4) = -x_1^4 \alpha^4 + \text{order}[\alpha^5], \quad (C19a)$$

$$D(x_4) = x_1^3 (f_1 - x_1) \alpha^4 / f + \text{order}[\alpha^5]. \quad (C19b)$$

Hence

$$M_{y,DP} = \frac{-x_4}{x_1} = \frac{-N/D}{x_1} = \frac{1}{x_1} \frac{x_1^4 + \text{order}[\alpha]}{x_1^3 (f - x_1) / f + \text{order}[\alpha]} \xrightarrow{\alpha=0} \frac{1}{1 - x_1/f}, \quad (C20)$$

which, in terms of ϵ'' , is

$$M_{y,DP} = \frac{1}{(1 - 2\epsilon'')}. \quad (5)$$

The authors dedicate this paper to the late Ternay Neu of Surface Optics Corporation. The authors thank the Measurement Science Directorate of the Naval Warfare Assessment Division, Corona, Calif., for its support of this research.

References and Notes

1. J. A. Sanderson, "The diffuse reflectance of paints in the near infra-red," *J. Opt. Soc. Am.* **37**, 771–777 (1947).
2. W. L. Derksen, T. I. Monahan, and A. J. Lawes, "Automatic recording reflectometer for measuring diffuse reflectance in the visible and infrared regions," *J. Opt. Soc. Am.* **47**, 995–999 (1957).
3. R. V. Dunkle, "Spectral reflectance measurements," in *Surface Effects on Spacecraft Materials*, F. J. Clauss, ed. (Wiley, New York, 1960), p. 117.
4. S. T. Dunn, J. C. Richmond, and J. A. Wiebelt, "Ellipsoidal mirror reflectometer," *J. Res. Natl. Bur. Stand. Sec. C* **70**, 75–88 (1966).
5. J. T. Neu, "Design, fabrication and performance of an ellipsoidal spectrorreflectometer," Rep. NASA-CR-73193 (National Aeronautics and Space Administration, Washington, D.C., 1968).
6. R. P. Heinisch, F. J. Bradac, and D. B. Perlick, "On the fabrication and evaluation of an integrating hemiellipsoid," *Appl. Opt.* **9**, 483–487 (1970).
7. B. E. Wood, J. G. Pipes, A. M. Smith, and J. A. Roux, "Hemiellipsoidal mirror infrared reflectometer: development and operation," *Appl. Opt.* **15**, 940–950 (1976).
8. F. J. J. Clarke, "Measurement of the radiometric properties of materials for building and aerospace applications," *Proc. SPIE* **234**, 40–47 (1980).
9. W. W. Coblenz, "The diffuse reflectance power of various substances," *Bull. Bur. Stand. (V. S.) Bull.* **9**, 283–325 (1913).
10. J. M. Bennett and L. Mattson, *Introduction to Surface Roughness and Scattering* (Optical Society of America, Washington, D.C. 1989).
11. R. R. Willey, "Fourier transform infrared spectrophotometer for transmittance and diffuse reflectance measurements," *Appl. Spectrosc.* **30**, 593–595 (1976).
12. W. Richter, "Fourier transform reflectance spectrometry between 8000 cm^{-1} ($1.25\text{ }\mu\text{m}$) and 800 cm^{-1} ($12.5\text{ }\mu\text{m}$) using an integrating sphere," *Appl. Spectrosc.* **37**, 32–38 (1983).
13. U. P. Oppenheim, M. G. Turner, and W. L. Wolfe, "BRDF reference standards for the infrared," *Infrared Phys. Technol.* **35**, 873–879 (1994).
14. K. A. Snail and L. M. Hanssen, "Reflectance measurements using conic mirror reflectometers," in *Applied Spectroscopy: A Compact Reference for Practitioners*, J. Workman and A. Springsteen, eds. (Academic, San Diego, Calif., 1998).
15. F. J. J. Clarke and D. J. Parry, "Helmholtz reciprocity: its validity and application to reflectometry," *Lighting Res. Technol.* **17**, 1–11 (1985).
16. W. Richter and W. Erb, "Accurate diffuse reflectance measurements in the infrared," *Appl. Opt.* **26**, 4620–4624 (1987).
17. W. M. Brandenburg, "Focussing properties of hemispherical and ellipsoidal mirror reflectometers," *J. Opt. Soc. Am.* **54**, 1235–1237 (1964).
18. D. K. Edwards, "Comments on reciprocal-mode 2π -sr-mirror reflectometers," *Appl. Opt.* **5**, 175–176 (1966).
19. P. R. Griffiths and J. A. de Haseth, *Fourier Transform Infrared Spectroscopy* (Wiley, New York, 1986).
20. K. A. Snail, "Reflectometer design using nonimaging optics," *Appl. Opt.* **26**, 5326–5332 (1987).
21. The ray tracing was performed with the Advanced Stray Light Analysis Package (ASAP) from Breault Research Organization, Tucson, Ariz. Maximum magnification runs used rays traced in double precision at an angle of 89.9° .
22. F. Paschen, "Über die Vertheilung der Energie im Spectrum des schwarzen Körpers bei niederen temperaturen," *Berl. Akad. Wiss.* **22**, 405–420 (1899).